Hemiasterlin derivative *(R)(S)(S)*-BF65 and Akt inhibitor MK-2206 synergistically inhibit SKOV3 ovarian cancer cell growth

Wei-Ting Lai [a], Kai-Lin Cheng [a], Riccardo Baruchello [b], Riccardo Rondanin [b], Paolo Marchetti [b], Daniele Simoni [b], Ray M. Lee [c], Jih-Hwa Guh [a], Lih-Ching Hsu [a]*

[a] School of Pharmacy, College of Medicine, National Taiwan University, No. 33, Linsen S. Road, Taipei 10050, Taiwan

[b] Department of Pharmaceutical Sciences, University of Ferrara, Via Fossato di Mortara 17/19, 44121, Ferrara, Italy

[c] Lestoni Corp, Richmond, VA, U.S.A.

*Corresponding author. Address: School of Pharmacy, National Taiwan University, No. 33, Linsen S. Road, Taipei 10050, Taiwan. Phone: +886-2-3366-8759; Fax: +886-2-2391-9098.

E-mail address: lhsu@ntu.edu.tw

Abstract

We reported previously that a hemiasterlin derivative BF65 is a potent anticancer agent that can inhibit microtubule assembly. Here we show that a more potent stereospecific diastereomer *(R)(S)(S)*-BF65 can synergize with an allosteric Akt inhibitor MK-2206 to suppress the growth of SKOV3 ovarian cancer cells with constitutively active Akt. *(R)(S)(S)*-BF65 induced mitotic arrest and MK-2206 caused G0/G1 arrest, while the combination of both induced simultaneous G0/G1 and G2/M cell cycle arrest. *(R)(S)(S)*-BF65 induced phosphorylation and inactivation of Bcl-2, downregulated Mcl-1 and caused PARP cleavage, leading to apoptosis. *(R)(S)(S)*-BF65 inhibited mitogen-activated protein kinases (MAPKs), which may stimulate cell proliferation upon activation. *(R)(S)(S)*-BF65 also induced DNA damage after long-term treatment. MK-2206 is known to inhibit phosphorylation and activation of Akt and suppress cancer cell growth. The combination of *(R)(S)(S)*-BF65 and MK-2206 also inhibited phosphorylation of Akt and its downstream effectors. Interestingly, MK-2206 upregulated Bcl-2 in SKOV3 cells; however, when combined with *(R)(S)(S)*-BF65, Bcl-2 protein induced by MK-2206 was phosphorylated and inactivated. The combination also more significantly decreased Mcl-1 protein, increased PARP cleavage, and induced γ-H2AX, a DNA damage marker. *(R)(S)(S)*-BF65 inhibited phosphorylation of MAPKs, which in turn blocked activation of the MAPK pathway resulting from feedback of Akt inhibition by MK-2206. Remarkably, MK-2206 enhanced the microtubule depolymerization effect of *(R)(S)(S)*-BF65. The combination of *(R)(S)(S)*-BF65 and MK-2206 also markedly inhibited cell migration. These molecular changes may explain why *(R)(S)(S)*-BF65 can synergize with MK-2206 to inhibit SKOV3 ovarian cancer cell growth and enhance cytotoxicity, and suggest that the combination may also suppress cancer cell invasion.

Keywords: hemiasterlin derivative *(R)(S)(S)*-BF65, Akt inhibitor MK-2206, MAPK and Akt signaling pathways, ovarian cancer

1. Introduction

Ovarian cancer, a deadly gynecologic cancer and the fifth leading cause of cancer death in women, is usually diagnosed at advanced stages with a very poor survival rate. The standard treatment for advanced ovarian cancer is surgical tumor debulking followed by chemotherapy typically includes taxanes, such as paclitaxel (Taxol), which can stabilize microtubule assembly to abolish dynamic function of microtubules, induce mitotic arrest, and cause growth arrest and apoptosis [1,2].

Antimicrotubule agents are frequently used in first-line chemotherapy. Other than taxanes, vinca alkaloids including vincristine, vinblastine and vinorelbine which can inhibit tubulin polymerization, have been used for the treatment of a variety of cancers [3]. However, these antimicrotubule agents are substrates of ATP-dependent drug efflux pumps known as ABC-transporters, such as the multidrug resistance efflux pump P-glycoprotein, and patients tend to develop drug resistance due to overexpression of these transporters in tumor cells [3]. Hemiasterlins are a group of cytotoxic tripeptides with antimicrotubule activity originally isolated from marine sponges. These small peptides have been shown to inhibit microtubule assembly and several synthetic analogs, such as HTI-286 (taltobulin) and E7974, are in clinical development as anticancer agents [4,5]. Unlike other antimicrotubule agents in clinical use, hemiasterlin derivatives HTI-286 and E7974 are poor substrates for P-glycoprotein and can circumvent drug resistance associated with this efflux pump [4,5]. We have synthesized a series of hemiasterlin derivatives and demonstrated that one of the derivative BF65, which contains a mixture of *(R)(S)(S)* and *(S)(S)(S)* diastereomers, displays a potent cytotoxic activity towards a panel of cancer cell lines including ovarian cancer, lung cancer, breast cancer, colon cancer, pancreatic cancer and hepatocellular carcinoma. Like other antimicrotubule agents, BF65 induces mitotic arrest and cell death in the low nanomolar range [6].

Antimicrotubule agents cause mitotic arrest and apoptosis by modulating phosphorylation of pro-survival protein Bcl-2, cell cycle-related kinase Cdc2 and mitogen-activated protein kinases (MAPKs) [7–9]. Mitosis is regulated by the cyclin B/Cdc2 complex. Cyclin B1 levels oscillate during the cell cycle and a large amount of cyclin B1 is expressed just prior to mitosis; whereas, the levels of Cdc2 remain constant. The cyclin B/Cdc2 complex is inactive in G2 when Cdc2 is inactivated by phosphorylation at Thr14 and Tyr15. During G2/M transition, the Cdc25C phosphatase is activated by Polo-like kinase 1 (PLK1), which in turn dephosphorylates and activates Cdc2, thereby promoting mitotic entry [10]. We have shown previously that BF65, like vincristine, induced dephosphorylation of Cdc2 at Thr14 and Cdc25C at Ser216 (also an inhibitory phosphorylation site), indicative of their activation and mitosis entry. Bcl-2 phosphorylation, which leads to its inactivation, and cleavage of caspase 3 were also induced by these antimicrotubule agents, leading to apoptosis [6]. MAPK pathways, including extracellular signal-regulated kinase (ERK), p38 and c-Jun N-terminal kinase (JNK), play an important role in the regulation of cellular processes such as cell proliferation, differentiation and apoptosis [9,11]. It has been reported that MAPKs can be activated or inhibited by antimicrotubule agents such as paclitaxel, vincristine and vinblastine, and the effect is associated with apoptosis induction. The differential effect of microtubule-targeting agents on MAPKs may depend on whether the agent promotes microtubule polymerization or depolymerization or may be cell line specific [7,12].

Abnormalities in the phosphatidylinositol-3-kinase (PI3K)/Akt pathway including amplification or activating mutations of the *PIK3CA* gene, overactivation of the serine/threonine kinase Akt, or loss of PTEN tumor suppressor function are frequently observed in human cancers [13]. Akt can activate its downstream serine/threonine kinase mammalian target of rapamycin (mTOR), which can phosphorylate p70 ribosomal protein kinase (p70S6K) and 4E-binding protein 1 (4E-BP1). Phosphorylation of 4E-BP1 results in the release of translation initiation factor eIF4E and induction of

protein translation. Deregulation of this pathway may enhance cell survival, increase proliferation, suppress apoptosis and contribute to neoplastic transformation [13]. Moreover, constitutive activation of this pathway is also associated with resistance to conventional chemotherapy [14]. Therefore, targeting the PI3K/Akt pathway is considered to be a promising strategy for cancer therapy and for overcoming chemotherapy resistance.

MK-2206, an allosteric Akt inhibitor under development for the treatment of solid tumors, can block the phosphorylation and activation of Akt. It has been reported that MK-2206 synergistically inhibit proliferation of many human cancer cell lines, and suppress tumor growth in mouse xenograft models, when combined with molecular targeted agents such as erlotinib and lapatinib, or cytotoxic agents such as docetaxel and carboplatin [15]. Mechanisms underlying cytotoxicity of MK-2206 include inhibition of Akt activation, induction of reactive oxygen species, and cross-talk between autophagy and apoptosis [15–17]. *PIK3CA* gene amplification and Akt activation have been frequently found in ovarian cancers [13,18]. Thus, Akt is a potential molecular target for the treatment of ovarian cancer and clinical trials of MK-2206 in ovarian cancer are in progress.

To better manage ovarian cancer, novel treatment strategies are in need to improve the treatment efficacy and to circumvent drug resistance. We have recently demonstrated that MK-2206 can synergistically enhance the cytotoxic effect of both paclitaxel and cisplatin in human ovarian cancer cell lines SKOV3 and ES-2 [19]. MK-2206 showed a better synergistic cytotoxic effect when combined with paclitaxel or cisplatin in SKOV3 cells which express constitutively active Akt than ES-2 cells with no active Akt [19]. SKOV3 cells carry a *PIK3CA* H1047R mutation that leads to constitutive Akt activation and the *p53* gene is homozygously mutated [15,20]. In a previous study, we found that the *(R)(S)(S)*-BF65 was much more potent than *(S)(S)(S)*-BF65 [21]. Since hemiasterlins are promising anticancer agents without drug resistance issue associated with the multidrug resistance efflux pumps, we thus used SKOV3 as a cell model for ovarian cancer with Akt overactivation and

p53 deficiency to investigate whether the more potent hemiasterlin derivative *(R)(S)(S)*-BF65, when combined with MK-2206, exerted a synergistic cytotoxic effect, and sought to dissect the underlying molecular mechanisms.

2. Materials and Methods

2.1. Chemicals

MK-2206 was purchased from BioVision (Mountain View, CA). 3-(4,5-Dimethylthiazol-2-yl)-2,5-diphenyltetrazolium bromide (MTT) and propidium iodide (PI) were obtained from Invitrogen Life Technologies (Carlsbad, CA). Trichloroacetic acid (TCA), sulforhodamine B (SRB) and vincristine were purchased from Sigma-Aldrich (St. Louis, MO). U0126 was purchased from Cell Signaling Technologies (Boston, MA). Stock solutions of MK-2206, *(R)(S)(S)*-BF65, *(S)(S)(S)*-BF65, vincristine and U0126 were prepared in DMSO, MTT was dissolved in PBS (5 mg/ml), and 0.4% (w/v) SRB solution was prepared in 1% acetic acid.

2.2. Cell culture, drug treatment and cell viability assays

Human ovarian cancer cells SKOV3 (ATCC HTB-77) were grown in McCoy's 5A medium supplemented with 10% fetal bovine serum and 1.5 mM L-glutamine at 37ºC in a humidified 5% CO_2 atmosphere. Cells were seeded in 96-well plates (2.5-3.5 x 10^3 cells/well) and subjected to drug treatments for indicated time periods followed by the MTT or SRB assay to measure cell growth as described previously [19,22]. Absorbance was measured at 570 nm with a reference wavelength of 690 nm for the MTT assay and at 515 nm for the SRB assay.

2.3. Combination index analysis

Combination index (CI), an indicator of drug interactions in combination chemotherapy, is calculated according to the following formula:

$CI = C_{A,X}/ IC_{X,A} + C_{B,X}/ IC_{X,B}$

$C_{A,X}$ and $C_{B,X}$ represent the concentrations of drug A and drug B, when used in combination to achieve x% drug effect. $IC_{X,A}$ and $IC_{X,B}$ are the concentrations required for individual treatments to achieve the same x% effect. CI < 1 indicates synergy, CI = 1 denotes an additive effect, and CI > 1 represents antagonism [23,24].

2.4. Flow cytometric analysis

Cells were treated with drugs, harvested by trypsinization and fixed in 75% ethanol for 30 min to overnight at -20^{o}C, and then subjected to PI staining and flow cytometric analysis. At least 10,000 cells were analyzed for each sample using CellQuest Pro software (BD Biosciences, San Jose, CA).

2.5. Western blot analysis

After drug treatment, cells were harvested and lysed in a lysis buffer containing 20 mM Tris-HCl,pH 7.4, 150 mM NaCl, 1% Triton X-100, 1 mM EDTA, 1 mM EGTA, protease inhibitor cocktail (Roche Diagnostics, Indianapolis, IN), 1 μg/ml pepstain A, 50 mM sodium fluoride, and 1 mM sodium orthovanadate. Cleared cell lysates containing 20 μg of protein were subjected to 7.5% or 12% SDS-PAGE and Western analysis as described [25]. Primary antibodies used were Phospho-Akt (Ser473), total Akt, phospho-Cdc2 (Thr14), phospho-Cdc25C (Ser216), phospho-ERK (Thr202/Tyr204), phospho-p38 (Thr180/Tyr182), phospho-JNK (Thr183/Tyr185), phospho-p70S6K (Thr389), phospho-4E-BP1 (Thr37/46) (purchased from Cell Signaling, Boston, MA), Bak, cyclin B1, Mcl-1, PLK1 (Santa Cruz Biotechnology, Santa Cruz, CA), Bcl-2 (Dako, Carpinteria, CA), LC3

(Novus Biologicals, Littleton, CO), PARP (BD Biosciences, San Jose, CA), MPM2, p-Histone H3 (Ser10), γ-H2AX (S139)(Millipore, Billerica, MA), and γ-tubulin (Sigma-Aldrich, St. Louis, MO).

2.6. Immunofluorescence staining

Cells were plated into 8-well chamber slides (~2 x 10^4 cells/well), cultured for 24 h, and left untreated or treated with *(R)(S)(S)*-BF65, vincristine or MK-2206 alone or in combination for 24 h. Cells were then fixed in cold methanol for 5-10 min at -20ºC, permeabilized for 5-10 min at room temperature in a Tris-buffered saline containing 0.2% Triton X-100, and subjected to immunofluorescence staining as described previously [25]. The primary antibody used was α-tubulin DM1A (1:500 dilution, Sigma-Aldrich, St. Louis, MO) and the secondary antibody used was FITC-conjugated anti-mouse IgG (1:200 dilution). Nuclear counter-staining was performed using DAPI and the slides were mounted with antifade (Invitrogen, Carlsbad, CA). Images were captured using a Zeiss Axioscope A1 upright fluorescence microscope with a 40x objective (Carl Zeiss GmbH, Jena, Germany).

2.7. DNA fragmentation assay

Cells were plated into a 24-well plate (~3 x 10^4 cells/well) one day before drug treatment and pretreated with vehicle (DMSO) or 10 μM MEK inhibitor U0126 for 30 min, and then 20 μM MK-2206 was added. The treatment was carried out for 24 h and cells were subjected to DNA fragmentation assay using the Cell Death Detection ELISA^{PLUS} kit according to the manufacturer's instructions (Roche Applied Science, Mannheim, Germany). This *in vitro* assay determines apoptosis by quantitatively measuring mono- and oligonucleosomes. Briefly, cells were lysed and the cleared lysates were incubated with a mixture of biotin-conjugated anti-histone and peroxidase-conjugated anti-DNA in a streptavidin-coated microplate for 2 h at room temperature. After washing in incubation

buffer, ABTS substrate was added to photometrically determine the amount of peroxdase retained in the immunocomplex. Absorbance was measured at 405 nm using 490 nm as a reference wavelength. The degree of apoptosis was calculated by dividing the absorbance of a drug treated sample by that of the untreated control.

2.8. Wound healing assay

Cells were plated into 24-well plates (5 x 10^4 cells/well) and cultured for 2-3 days until the cell density reached 100% and then a scratch was made in the monolayer cells using a pipette tip. Culture medium was replaced with that containing vehicle (DMSO), 5 μM MK-2205, 10 nM *(R)(S)(S)*-BF65, 10 nM vincristive, or a combination of MK-2205 and *(R)(S)(S)*-BF65 or vincristive. Wound healing was monitored over a time course and imaged using an Olympus CKX41 inverted microscope with a 10x objective. The gap between both sides of the scratch was measured in 6 locations for each sample and the average of which was used for the calculation of % wound healing.

2.9. Statistical analysis

Results were presented as mean ± standard error (SE). Statistical significance was assessed with two-sided *t*-tests, and *p*-values less than 0.05 ($p< 0.05$) were considered statistically significant.

3. Results

3.1. (R)(S)(S)-BF65 and MK-2206 synergistically inhibit SKOV3 cell growth

We previously reported that a synthetic hemiasterlin derivative BF65, which is a mixture of *(R)(S)(S)*-BF65 and *(S)(S)(S)*-BF65 diastereomers, displayed potent anticancer activity towards a panel of cancer cell lines [6] and we also demonstrated that *(R)(S)(S)*-BF65 was more potent than

(S)(S)(S)-BF65 in an ovarian cancer cell line UCI-101 [21]. Here we first determined the 50% inhibitory concentration (IC_{50}) values of *(R)(S)(S)*-BF65 and *(S)(S)(S)*-BF65 (chemical structures shown in Fig. 1A) in SKOV3 ovarian cancer cells treated for 48 h and the values were 5.67 ± 1.07 nM and 144 ± 25.2 nM respectively (mean ± SE of three independent experiments), confirming that *(R)(S)(S)*-BF65 is the active component of BF65. *(R)(S)(S)*-BF65 was then used in the subsequent studies and abbreviated as BF65 in the figures for simplicity.

It has been demonstrated that the synergistic cytotoxic effect of MK-2206 and taxanes is sequence-dependent with a better synergy when docetaxel or paclitaxel is administered prior to MK-2206 [15,19]. To determine whether a combination of *(R)(S)(S)*-BF65 and MK-2206 had a synergistic cytotoxic effect on ovarian cancer cells, we first tested three treatment sequences in SKOV3 cells: *(R)(S)(S)*-BF65 for 24 h followed by MK-2206 for 72 h (BF65 24 h→MK-2206 72 h), cotreatment with *(R)(S)(S)*-BF65 and MK-2206 for 96 h (BF65+MK-2206 96 h), and MK-2206 for 24 h followed by *(R)(S)(S)*-BF65 for 72 h (MK-2206 24 h→BF65 72 h). The concentrations of *(R)(S)(S)*-BF65 ranged from 0-50 nM and MK-2206 from 0-25 μM, and the concentration ratio of *(R)(S)(S)*-BF65 and MK-2206 was 1:500, the same as the ratio for paclitaxel and MK-2206 in a previous study [19]. MTT and SRB assays were used to evaluate cell viability. A set of representative dose-response curves of single and combination treatments of the three sequences obtained from the MTT assay are illustrated in Fig. 1 B-D. The IC_{50} and combination index at IC_{50} (CI_{50}) values, calculated from three independent experiments, indicated that *(R)(S)(S)*-BF65 and MK-2206 displayed a synergistic cytotoxic effect in all three treatment sequences (Fig. 1E). The CI_{50} values were 0.92, 0.78 and 0.91 respectively for BF65 24 h→MK-2206 72 h, BF65+MK-2206 96 h, and MK-2206 24 h→BF65 72 h. Cotreatment of SKOV3 cells with *(R)(S)(S)*-BF65 and MK-2206 for 96 h showed the best synergy and cell viability of this combination treatment was significantly lower than either single treatment of *(R)(S)(S)*-BF65 or MK-2206 at each concentration except the highest concentration of

MK-2206 (25 μM)(Fig. 1C). The SRB assay was also used to evaluate cell viability and similar dose-response curves were obtained (Fig. S1) and the CI_{90} values were 0.42, 0.47 and 0.94 respectively for BF65 24 h→MK-2206 72 h, BF65+MK-2206 96 h, and MK-2206 24 h→BF65 72 h (Fig. 1F).

In the cotreatment groups, IC_{50} values of *(R)(S)(S)*-BF65 and MK-2206 were 8.9 nM and 5.7 μM respectively in single treatments, 3.9 nM and 1.95 μM in cotreatment (CI_{50} = 0.78)(Fig. 1E); and IC_{90} values of *(R)(S)(S)*-BF65 and MK-2206 were 19 nM and 12 μM respectively in single treatments, 4.95 nM and 2.47 μM in cotreatment (CI_{90} = 0.47)(Fig. 1F). The cotreatment sequence was then chosen for further investigation of the molecular mechanisms underlying the synergy of *(R)(S)(S)*-BF65 and MK-2206.

3.2. The combination of (R)(S)(S)-BF65 and MK-2206 induces G0/G1, G2/M arrest, and apoptosis

It has been reported that MK-2206 induces G1 arrest [26,27]. We have demonstrated previously that BF65 causes M phase arrest [6]. To evaluate the combinatorial effect of *(R)(S)(S)*-BF65 and MK-2206 on cell cycle progression, SKOV3 cells were untreated (Control) or treated with 5, 20 or 40 nM of *(R)(S)(S)*-BF65 and 2.5, 10 or 20 μM of MK-2206 either alone or in combination for 24 or 48 h and subjected to flow cytometric analysis. Similar results were obtained for 24 and 48 h. Representative results of the cell cycle distribution from the 24 h time point are illustrated in Fig. 2A, and the G0/G1 and G2/M populations at both 24 and 48 h, calculated from three independent experiments, are shown in Fig. 2B. *(R)(S)(S)*-BF65 alone clearly induced G2/M arrest in a dose-dependent manner, and up to 80% of cells arrested at G2/M after treated with 40 nM of *(R)(S)(S)*-BF65 for 24 or 48 h (only ~18% in the untreated control); whereas, the G0/G1 populations were dramatically diminished (Fig. 2). MK-2206 alone increased the G0/G1 population within 24 h and the G0/G1 population reached 80% at 48 h (72% in the untreated control) with S phase cells

clearly diminished (Fig. 2). Interestingly, the combination of *(R)(S)(S)*-BF65 and MK-2206 resulted in accumulation of cells in both G0/G1 and G2/M (Fig. 2).

The cell cycle effects of 40 nM *(R)(S)(S)*-BF65, 20 μM MK-2206, and the combination of both were then determined over a time course from 6 h to 96 h. Representative results of the cell cycle distribution are illustrated in Fig. 3A and quantitative data of subG1, G0/G1, G2/M, and > 4n cell populations from 2-3 independent experiments are shown in Fig. 3B-E. *(R)(S)(S)*-BF65 alone induced marked accumulation of G2/M cells within 24-48 h (81-82%), and then the G2/M peaks dwindled (49% at 72 h and 38% at 96 h) accompanied with increasing subG1 populations (~30%) and the advent of cells with an 8n DNA content at 72 and 96 h (Fig. 3). Treatment with 20 μM MK-2206 resulted in clear accumulation of G0/G1 cells within 24-48 h (72% at 24 h and 80% at 48 h), then the G0/G1 populations were decreased (67% at 72 h and 51% at 96 h) and subG1 populations were increased (20% at 72 h and 41% at 96 h), with the S phase (Fig. 3A) and G2/M populations diminishing over time (Fig. 3). The combination of *(R)(S)(S)*-BF65 and MK-2206 caused accumulation of G0/G1 and G2/M cells within 24 h and then both G0/G1 and G2/M peaks decreased from 48 to 96 h with a concomitant increase in the subG1 population. The subG1 population was higher in the combination group compared to single agents, and a synergistic effect was observed at the 48 h time point. The % subG1 of 40 nM *(R)(S)(S)*-BF65, 20 μM MK-2206, and the *(R)(S)(S)*-BF65+MK-2206 combination were 10.8 ± 1.90, 3.87 ± 1.33, and 15.5 ± 2.14, respectively ($P = 0.032$, *(R)(S)(S)*-BF65 vs. combination; $P = 0.0053$, MK-2206 vs. combination, 2-sided *t*-test)(Fig. 3B). Intriguingly, the 8n peak induced by extended treatment with 40 nM *(R)(S)(S)*-BF65 disappeared when *(R)(S)(S)*-BF65 was combined with 20 μM MK-2206 (Fig. 3A). The > 4n population induced by 40 nM *(R)(S)(S)*-BF65 at 96 h was significantly suppressed in the presence of 20 μM MK-2206 (28.8 ± 4.22% vs. 2.94 ± 0.14%, $P = 0.026$, 2-sided *t*-test)(Fig. 3E). Although the

combination of *(R)(S)(S)*-BF65 and MK-2206 also arrested cells in G2/M and G0/G1, they did antagonize the cell cycle effect of each other (Fig. 3, C and D).

3.3. The effects of (R)(S)(S)-BF65 on proteins associated with G2/M progression, cell death, DNA damage and the MAPK signaling pathway

To further investigate the underlying molecular mechanisms, SKOV3 cells were treated with 0, 10, 20, or 40 nM of *(R)(S)(S)*-BF65 for 24, 48, and 72 h and subjected to Western analysis. MPM2, PLK1, cyclin B1 and phosphorylated histone H3 (p-Histone H3) at Ser10 are associated with G2/M cell cycle progression, and their levels are increased in mitosis. As illustrated in Fig. 4, MPM2, PLK1, cyclin B1 and p-Histone H3 levels were markedly induced by treatment with *(R)(S)(S)*-BF65 for 24 and 48 h, but the induction was declined after extended treatment (Fig. 4A) concurrent with the appearance of PARP cleavage at 72 h (Fig. 4B), indicating that some cells had undergone apoptosis. Inhibitory phosphorylation of Cdc2 (p-Cdc2) at Thr14 and Cdc25C (p-Cdc25C) at Ser216 was decreased dose-dependently after *(R)(S)(S)*-BF65 treatment, indicative of their activation which led to mitotic entry (Fig. 4A).

As shown in Fig. 4B, *(R)(S)(S)*-BF65 downregulated anti-apoptotic Mcl-1 and induced Bcl-2 phosphorylation in a dose-dependent manner, but pro-apoptotic Bak protein levels were not much affected. Thus, downregulation or inactivation of pro-survival proteins may contribute to *(R)(S)(S)*-BF65-induced cell death. It has been reported that vinca alkaloids cause DNA damage which may subsequently result in apoptosis in lung adenocarcinoma cells [28]. At 72 h, *(R)(S)(S)*-BF65 also induced γ-H2AX, a DNA damage marker. These results suggest that extended treatment with *(R)(S)(S)*-BF65 may induce DNA damage leading to apoptosis.

Antimicrotubule agents may inhibit or activate MAPKs, which is associated with the induction of apoptosis [7,12]. We then determined the effect of *(R)(S)(S)*-BF65 on the levels of phosphorylated

MAPKs, including ERK, p38, and JNK, which represent their active forms, in SKOV3 cells. *(R)(S)(S)*-BF65 did not have a clear effect on phosphorylation of JNK at Thr183/Tyr185 (data not shown); however, it downregulated phosphorylation of ERK at Thr202/Tyr204 and p38 at Thr180/Tyr182 in a dose-dependent fashion as shown in Fig. 4B. Interestingly, when another ovarian cancer cell line UCI-101 was treated with 100 nM of BF65 for up to 36 h, no significant changes in p-ERK was observed, suggesting that the effect of BF65 or *(R)(S)(S)*-BF65 on the activation of the MAPK pathway could be cell-type specific [6].

Altogether, these results confirmed that *(R)(S)(S)*-BF65 arrested SKOV3 ovarian cancer cells in M phase and may eventually induce apoptosis via downregulation of Mcl-1, induction of Bcl-2 phosphorylation, induction of DNA damage, as well as inhibition of MAPKs, p38 and ERK.

3.4. Combinatorial effects of (R)(S)(S)-BF65 and MK-2206 on proteins related to G2/M progression, cell death, and the Akt and MAPK signaling pathways

To elucidate the molecular mechanisms underlying the synergistic growth inhibitory and cytotoxic effects of *(R)(S)(S)*-BF65 and MK-2206, SKOV3 cells were treated with 10 or 40 nM *(R)(S)(S)*-BF65 and 5 or 20 μM MK-2206 either alone or in combination for 24 or 48 h, and proteins associated with G2/M cell cycle progression, cell death, as well as the Akt and MAPK signaling pathways were analyzed. As shown in Fig. 5A, single treatment with 10 or 40 nM *(R)(S)(S)*-BF65 increased the levels of mitosis-related proteins PLK1, cyclin B1 and p-histone H3 as in Fig. 4A. MK-2206 single treatment downregulated PLK1 levels as compared to the untreated controls (Fig. 5A). In the 10 nM *(R)(S)(S)*-BF65 + 5 μM MK-2206 combination, MK-2206 did not have a clear influence on mitosis-related proteins induced by 10 nM *(R)(S)(S)*-BF65 at 24 h. However, as the concentrations and treatment time periods increased, MK-2206 counteracted the effect of *(R)(S)(S)*-BF65 and decreased the levels of PLK1, cyclin B1 and p-histone H3 induced by *(R)(S)(S)*-BF65 at various

degrees (Fig. 5A), consistent with the flow cytometric data in Fig. 1 and Fig. 2 showing that MK-2206 somewhat mitigated mitotic arrest by *(R)(S)(S)*-BF65.

MK-2206 effectively blocked phosphorylation and activation of Akt and also downregulated phosphorylation of its downstream effectors p70S6K and 4E-BP1 time- and dose-dependently (Fig 5A). *(R)(S)(S)*-BF65 alone slightly enhanced the levels of p-p70S6K and p-4E-BP1 but had no obvious effect on pAkt. The addition of *(R)(S)(S)*-BF65 to MK-2206 showed intermediate effects at low doses or early time point; but in the 40 nM *(R)(S)(S)*-BF65 + 20 μM MK-2206 combination, the suppression of p-Akt, p-p70S6K and p-4E-BP1 levels was significantly enhanced with p-Akt, p-p70S6K and p-4E-BP1 levels downregulated by 40% ($P = 0.014$, n = 2), 50% ($P = 0.036$, n = 3), or 39% ($P = 0.0016$, n = 3) respectively compared to 20 μM MK-2206 alone at 48 h (Fig. 5A).

Compared to *(R)(S)(S)*-BF65 alone (Fig. 4B and Fig. 5B), PARP cleavage occurred earlier and was more profound when *(R)(S)(S)*-BF65 was combined with MK-2206 (Fig. 5B). *(R)(S)(S)*-BF65 alone downregulated Bcl-2 and Mcl-1. Interestingly, MK-2206 single treatment markedly induced Bcl-2. The addition of *(R)(S)(S)*-BF65 not only resulted in phosphorylation and inactivation of Bcl-2 but also further downregulated Mcl-1 most clearly in the 40 nM *(R)(S)(S)*-BF65 + 20 μM MK-2206 combination at 48 h. DNA damage was also enhanced in the *(R)(S)(S)*-BF65/MK-2206 combination as γ-H2AX was induced and exhibited a dramatic increase in the 40 nM *(R)(S)(S)*-BF65 + 20 μM MK-2206 combination at 48 h.

It has been reported that MK-2206 can induce both apoptosis and autophagy in glioma cells. Autophagy induced by MK-2206 is cytoprotective and suppression of autophagy augments its apoptotic effect [16,17]. We found that LC3 form II (LC3-II), an autophagy marker, was significantly induced by MK-2206 in a dose- and time-dependent manner in SKOV3 cells; however, this effect was not significantly affected when MK-2206 was combined with *(R)(S)(S)*-BF65 (Fig. 5B). Whether

autophagy induced by MK-2206 is associated with cell survival or apoptosis in SKOV3 remained to be clarified.

Intriguingly, MK-2206 induced phosphorylation and activation of ERK and p38 as well as JNK in SKOV3 cells, which could be a feedback mechanism due to inhibition of the Akt pathway. When combined with *(R)(S)(S)*-BF65, MK-2206-induced MAPK activation was significantly inhibited (Fig. 5B). This was consistent with the results shown in Fig. 4, indicating that *(R)(S)(S)*-BF65 could downregulate MAPKs (Fig. 4B).

All together, these data indicate that the combination of *(R)(S)(S)*-BF65 and MK-2206 may exert a synergistic cytotoxic effect in SKOV3 cells through modulating both the Akt and MAPK pathways. Remarkably, *(R)(S)(S)*-BF65 was able to counteract Bcl-2 upregulation and MAPK activation induced by MK-2206. Furthermore, the BF65/MK-2206 combination more significantly decreased Mcl-1 protein, increased PARP cleavage, and induced DNA damage.

3.5. MK-2206 enhances microtubule depolymerization effect of (R)(S)(S)-BF65

BF65 is a potent inhibitor of tubulin polymerization and has been demonstrated to induce abnormal mitotic cells with monopolar or multipolar spindles and microtubule depolymerization in interphase cells [6]. We next tested whether MK-2206 affected the microtubule depolymerization effect of *(R)(S)(S)*-BF65. SKOV3 cells were treated with 40 nM of *(R)(S)(S)*-BF65 and 20 μM of MK-2206 either alone or in combination for 24 h. As shown in Fig 6, 40 nM of *(R)(S)(S)*-BF65 clearly induced depolymerization of microtubules as well as accumulation of abnormal mitotic cells with multiple centrosomes. Cells treated with 20 μM MK-2206 alone displayed a normal microtubule pattern; however, when cotreated with 40 nM *(R)(S)(S)*-BF65 and 20 μM MK-2206, microtubule disruption was more effective compared to that caused by treatment with 40 nM *(R)(S)(S)*-BF65 alone. To test whether the enhancement of microtubule deplymerization by MK-2206 was specific for

(R)(S)(S)-BF65 or common to tubulin disrupting drugs, SKOV3 cells were also treated with 40 nM of vincristine alone or cotreated with 40 nM of vincristine and 20 μM of MK-2206, and a similar effect was observed (Fig. 6).

Since microtubules play a pivotal role in cell migration [29], we also performed the wound healing assay to evaluate the impact of the combination of MK-2206 with *(R)(S)(S)*-BF65 or vincristine on cell migration. As shown in Fig. 7A, the wound was approximately 100% healed within 24 h in untreated SKOV3 cells (C 24 h), and the gap was at least 50% filled in 5 μM MK-2206, 10 nM *(R)(S)(S)*-BF65 or 10 nM vincristine-treated cells. Significantly, wound healing was much less efficient in *(R)(S)(S)*-BF65/MK-2206 or vincristine/MK-2206-treated cells. Quantitative data obtained from multiple independent experiments is illustrated in Fig. 7B. The percentage of wound healing in the combination treatment was significantly lower than that in untreated control ($P < 0.001$) and single treatments ($P < 0.05$). Under the experimental conditions (5 μM MK-2206, 10 nM *(R)(S)(S)*-BF65 or 10 nM vincristine MK-2206), cell viability was similar in single and combination treatment groups, excluding a possibility that the impairment of wound healing was due to growth inhibition (data not shown).

Thus, MK-2206 enhances the microtubule depolymerization effect of *(R)(S)(S)*-BF65 as well as vincristine, and this effect may provide a rationale for combining MK-2206 with microtubule-destabilizing agents including hemiasterlins and the vinca alkaloids for cancer therapy. This combination more significantly inhibited cell migration, suggesting an inhibitory effect on cancer cell invasion and metastasis.

4. Discussion

In this report, we show that a hemiasterlin derivative *(R)(S)(S)*-BF65 synergizes with an allosteric Akt inhibitor MK-2206 to suppress the growth of SKOV3 ovarian cancer cells in all three treatment

sequences tested. However, cotreatment or *(R)(S)(S)*-BF65 prior to MK-2206 was better than MK-2206 treatment followed by*(R)(S)(S)*-BF65. *(R)(S)(S)*-BF65 exerts its cytotoxic effect via microtubule disruption and mitotic arrest whereas MK-2206 acts through G0/G1 arrest, raising a possibility that both agents may counteract the cytotoxic effect of each other. Indeed, cotreatment with *(R)(S)(S)*-BF65 and MK-2206 induced simultaneous G2/M and G0/G1 arrest but both populations were lower than those induced by single agents. However, the combination did cause enhanced apoptosis in SKOV3 cells. Interestingly, *(R)(S)(S)*-BF65 induced a 8n population after long-term treatment. The polypoid population may represent cells undergoing mitotic slippage and entering interphase without chromosome separation. These cells may survive and continue to proliferate, particularly in p53-deficient cells such as SKOV3 [10,30]. The addition of MK-2206 significantly reversed *(R)(S)(S)*-BF65-induced accumulation of polypoid popululation, which may lead to increased apoptosis; thus, may partly account for the synergistic cytotoxic effect of *(R)(S)(S)*-BF65 and MK-2206.

Chiu et al. have reported that vinca alkaloids induce M phase arrest in lung adenocarcinoma cells, which leads to accumulation of DNA damage and eventually apoptosis [28]. *(R)(S)(S)*-BF65 induced γ-H2AX, a DNA damage marker, after long-term treatment, suggesting that *(R)(S)(S)*-BF65 may exert anticancer effect via induction of DNA damage in SKOV3 cells. DNA damage was not only dramatically enhanced but also detected earlier when *(R)(S)(S)*-BF65 was combined with MK-2206. This effect may also in part contribute to the synergism.

Cross-talk between the PI3K/Akt and Ras/MAPK signaling pathways is context-dependent and both pathways can activate or inhibit each other [31]. It has been demonstrated that inhibition of Akt induces the expression and phosphorylation of receptor tyrosine kinases, which in turn may lead to activation of MAPKs such as ERK [32]. We found that MK-2206 induced phsophorylation of MAPKs particularly ERK, which could be due to feedback activation of MAPK signaling pathway upon

inhibition of Akt. ERK activation is usually associated with cell survival. Indeed, cell death assay revealed that when SKOV3 cells were pretreated with U0126, a MEK inhibitor which suppressed ERK activation, MK-2206-induced cell death was significantly enhanced suggesting that MK-2206-induced ERK activation is associated with cell survival (Fig. S2). Thus, suppression of MK-2206-induced ERK activation by *(R)(S)(S)*-BF65 may contribute to the synergistic cytotoxicity of the combination of *(R)(S)(S)*-BF65 and MK-2206 in SKOV3 cells.

Activation of the PI3K/Akt pathway can mediate cell survival in part by upregulation of Bcl-2 expression [33]. Surprisingly, Akt inhibitor MK-2206 markedly induced Bcl-2 which may compromise its cytotoxic effect in SKOV3 cells. By combining with *(R)(S)(S)*-BF65 which causes phosphorylation and inactivation of Bcl-2, the anticancer effect of MK-2206 can be greatly enhanced. We also observed that MK-2206 induced autophagy in SKOV3 cells within 24-48 h of treatment. It has been documented that MK-2206 induces autophagy in glioblastoma cell lines, which is cytoprotective [16] and by combining with gefitinib, autophagy can be further augmented at early stages but switched to apoptosis at late stages [17]. We found that the levels of autophagy marker, LC3-II, were significantly induced by MK-2206 in a dose-dependent manner; However, LC3-II levels were not much changed by the addition of *(R)(S)(S)*-BF65. Whether autophagy contributes to cytoprotection or apoptosis in SKOV3 cells remains unclear and requires further investigation.

We demonstrated that BF65 and a stilbene tubulin inhibitor displayed a synergistic cytotoxic effect which was correlated with enhanced tubulin depolymerization [6]. Here we show that the microtubule-disrupting effect of *(R)(S)(S)*-BF65 is dramatically enhanced by MK-2206 (Fig. 6), which may partly account for the synergistic cytotoxic effect. Microtubule-disrupting agents have been shown to affect cell migration [29]. Yang et al. have reported that high drug concentrations are needed to inhibit microtubule assembly and cell division, but low concentrations are sufficient to suppress dynamic instability and cell migration [34]. Furthermore, the PI3K/Akt signaling pathway also plays a

role in regulating cell motility [13]. In this report, we demonstrate for the first time that the combination of MK-2206 and *(R)(S)(S)*-BF65 at low concentrations (5 μM and 10 nM respectively) significantly inhibits migration of SKOV3 cells as revealed by the wound healing assay (Fig. 7), suggesting that this combination may suppress cancer invasion and metastasis. These microtubule-related effects of MK-2206 are not limited to the combination with *(R)(S)(S)*-BF65, but also with vincristine, providing a rationale for combining microtubule-disrupting agents and MK-2206. Future studies will test whether this combination can suppress cancer invasion/metastasis and whether it is effective to other cancer cell lines as well.

We have reported that MK-2206 enhanced cytotoxicity of paclitaxel and cisplatin in ovarian cancer cell lines SKOV3 cells which express constitutively active Akt and ES2 cells whose Akt is not phosphorylated and activated at all [19]. Further study indicated that the Akt inhibitor MK-2206 exerted the effect through different mechanisms in both cell lines and might have some off-target effects. Nevertheless, the synergism between MK-2206 paclitaxel or cisplatin was more significant in SKOV3 with constitutively activated Akt. Similarly, the combination of MK-2206 and *(R)(S)(S)*-BF65 was not as effective in ES2 cells as in SKOV3 cells (data not shown), supporting the idea that genetic background of cancer cells strongly influence responses to therapeutic drugs. The synergistic effect of the *(R)(S)(S)*-BF65 and MK-2206 in SKOV3 cells may provide a paradigm for ovarian cancer cells with Akt activation and p53 mutation, features commonly observed in human ovarian cancers [13,35]. However, more cell lines need to be examined to provide supporting evidence and further investigation is warranted.

In summary, MK-2206 synergizes with *(R)(S)(S)*-BF65 to inhibit SKOV3 cell growth via downregulating the Akt signaling pathway and enhancing the microtubule disruption effect of *(R)(S)(S)*-BF65. *(R)(S)(S)*-BF65 in turn suppresses Bcl-2 and MAPKs induced by MK-2206. The *(R)(S)(S)*-BF65/MK-2206 combination more significantly decreased Mcl-1 protein, increased PARP

cleavage, and induced DNA damage, eventually led to increased apoptosis and enhanced cytotoxicity, and may also suppress cancer cell invasion.

Acknowledgments

This study was supported by funds from the National Taiwan University (L.C.H.).

Conflict of Interest Statement

The authors declare that they have no conflict of interest.

References

[1] Berkenblit A, Cannistra SA. Advances in the management of epithelial ovarian cancer. J Reprod Med 2005;50:426–38.

[2] DiSaia PJ, Bloss JD, Treatment of ovarian cancer: new strategies. Gynecol Oncol 2003;90:S24–32.

[3] Jordan MA, Wilson L. Microtubules as a target for anticancer drugs. Nat Rev Cancer 2004;4:253–65.

[4] Loganzo F, Discafani CM, Annable T, Beyer C, Musto S, Hari M, et al. HTI-286, a synthetic analogue of the tripeptide hemiasterlin, is a potent antimicrotubule agent that circumvents P-glycoprotein-mediated resistance in vitro and in vivo. Cancer Res 2003;63:1838–45.

[5] Kuznetsov G, TenDyke K, Towle MJ, Cheng H, Liu J, Marsh JP, et al. Tubulin-based antimitotic mechanism of E7974, a novel analogue of the marine sponge natural product hemiasterlin. Mol Cancer Ther 2009;8:2852–60.

[6] Hsu LC, Durrant DE, Huang CC, Chi NW, Baruchello R, Rondanin R, et al. Development of hemiasterlin derivatives as potential anticancer agents that inhibit tubulin polymerization and synergize with a stilbene tubulin inhibitor. Invest New Drugs 2012;30:1379–88.

[7] Wang LG, Liu XM, Kreis W. Budman DR. The effect of antimicrotubule agents on signal transduction pathways of apoptosis: a review. Cancer Chemother Pharmacol 1999;44:355–61.

[8] Jackson JR, Patrick DR, Dar MM, Huang PS. Targeted anti-mitotic therapies: can we improve on tubulin agents? Nat Rev Cancer 2007;7:107–17.

[9] Dhillon AS, Hagan S, Rath O, Kolch W. MAP kinase signalling pathways in cancer. Oncogene 2007;26:3279–90.

[10] Castedo M, Perfettini JL, Roumier T, Andreau K, Medema R, Kroemer G. Cell death by mitotic catastrophe: a molecular definition. Oncogene 2004;23:2825–37.

[11] Zhang W, Liu HT. MAPK signal pathways in the regulation of cell proliferation in mammalian cells. Cell Res 2002;12:9–18.

[12] Stone AA, Chambers TC. Microtubule inhibitors elicit differential effects on MAP kinase (JNK, ERK, and p38) signaling pathways in human KB-3 carcinoma cells. Exp Cell Res 2000;254:110–9.

[13] Courtney KD, Corcoran RB, Engelman JA. The PI3K pathway as drug target in human cancer. J Clin Oncol 2010;28:1075–83.

[14] West KA, Castillo SS, Dennis PA. Activation of the PI3K/Akt pathway and chemotherapeutic resistance. Drug Resist Updat 2002;5:234–48.

[15] Hirai H, Sootome H, Nakatsuru Y, Miyama K, Taguchi S, Tsujioka K, et al. MK-2206, an allosteric Akt inhibitor, enhances antitumor efficacy by standard chemotherapeutic agents or molecular targeted drugs in vitro and in vivo. Mol Cancer Ther 2010;9:1956–67.

[16] Cheng Y, Ren X, Zhang Y, Patel R, Sharma A, Wu H, et al. eEF-2 kinase dictates crosstalk between autophagy and apoptosis induced by Akt inhibition, thereby modulating cytotoxicity of novel Akt inhibitor MK-2206. Cancer Res 2011;71:2654–63.

[17] Cheng Y, Zhang Y, Zhang L, Ren X, Huber-Keener KJ, Liu X, et al. MK-2206, a novel allosteric inhibitor of Akt, synergizes with gefitinib against malignant glioma via modulating both autophagy and apoptosis. Mol Cancer Ther 2012;11:154–64.

[18] Hanrahan AJ, Schultz N, Westfal ML. Sakr RA, Giri DD, Scarperi S, et al. Genomic complexity and AKT dependence in serous ovarian cancer. Cancer Discov 2012;2:56–67.

[19] Lin YH, Chen BYH, Lai WT, Wu SF, Guh JH, Cheng AL, et al. The Akt inhibitor MK-2206 enhances the cytotoxicity of paclitaxel (Taxol) and cisplatin in ovarian cancer cells. Naunyn-Schmiedebergs Arch Pharmacol 2015;388:19–31.

[20] Concin N, Stimpfl M, Zeillinger C, Wolff U, Hefler LJ, Sedlak J, et al. Role of p53 in G2/M cell cycle arrest and apoptosis in response to gamma-irradiation in ovarian carcinoma cell lines. Int J Oncol 2003;22:51–57.

[21] Simoni D, Lee RM, Durrant DE, Chi NW, Baruchello R, Rondanin R, Rullo C, Marchetti P. Versatile synthesis of new cytotoxic agents structurally related to hemiasterlins. Bioorg Med Chem Lett 2010;20:3431–5.

[22] Yu CC, Wu PJ, Hsu JL, Ho YF, Hsu LC, Chang YJ, et al. Apoptosis in human hormone-refractory prostate cancers through mitochondrial damage stress and survivin downregulation. Prostate 2013;73:133–45.

[23] Chou TC, Talalay P. Quantitative analysis of dose-effect relationships: the combined effects of multiple drugs or enzyme inhibitors. Adv Enzym Regul 1984;22:27–55.

[24] Zhao L, Wientjes MG, Au JL. Evaluation of combination chemotherapy: integration of nonlinear regression, curve shift, isobologram, and conbination index analyses. Clin Cancer Res 2004;10:7994–8004.

[25] Hsu LC, White RL. BRCA1 is associated with the centrosome during mitosis. Proc Natl Acad Sci USA 1998;95:12983–8.

[26] She QB, Chandarlapaty S, Ye Q, Lobo J, Haskell KM, Leander KR, et al. Breast tumor cells with PI3K mutation or HER2 amplification are selectively addicted to Akt signaling. PLoS One 2008;3:e3065.

[27] Jiao P, Zhou YS, Yang JX, Zhao YL, Liu QQ, Yuan C, et al. MK-2206 induces cell cycle arrest and apoptosis in HepG2 cells and sensitizes TRAIL-meditaed cell seath. Mol Cell Biochem 2013;382:217–24

[28] Chiu WH, Luo SJ, Chen CL, Cheng JH, Hsieh CY, Wang CY, et al. Vinca alkaloids cause aberrant ROS-mediated JNK activation, Mcl-1 downregulation, DNA damage, mitochondrial dysfunction, and apoptosis in lung adenocarcinoma cells. Biochem Pharmacol 2012;83:1159–71.

[29] Etienne-Manneville S. Microtubules in cell migration. Annu Rev Cell Dev Biol 2013;29:471–99.

[30] Vakifahmetoglu H, Olsson M, Zhivotovsky. Death through a tragedy: mitotic catastrophe. Oncogene 2008;15:1153–62.

[31] Aksamitiene E, Kiyatkin A, Kholodenko BN. Cross-talk between mitogenic Ras/MAPK and survival PI3K/Akt pathways: a fine balance. Biochem Soc Trans 2012;40:139–46.

[32] Chandarlapathy S, Sawai A, Scaltriti M, Rodrik-Outmezguine V, Grbovic-Huezo O, Serra V, et al. AKT inhibition relieves feedback suppression of receptor tyrosine kinase expression and activity. Cancer Cell 2011;19:58–71.

[33] Pugazhenthi S, Nesterova A, Sable C, Heidenreich KA, Boxer LM, Heasley LE, et al. Akt/protein kinase B up-regulates Bcl-2 expression through cAMP-response element-binding protein. J Biol Chem 2000;275:10761–6.

[34] Yang H, Ganguly A, Cabral F. Inhibition of cell migration and cell division correlates with distinct effects of microtubule inhibiting drugs. J Biol Chem 2010;285:32242–50.

[35] Cancer Genome Atlas Research Network. Integrated genomic analyses of ovarian carcinoma. Nature 2011;474:609–15.

Figure Legends

Fig. 1. The combination of *(R)(S)(S)*-BF65 and MK-2206 synergistically inhibits SKOV3 cell proliferation in three different treatment sequences. (A) Chemical structures of *(R)(S)(S)*-BF65 and *(S)(S)(S)*-BF65. The more active compound *(R)(S)(S)*-BF65 is marked with a *square* and abbreviated as BF65 in the figures. (B) Cells were treated with *(R)(S)(S)*-BF65 for 24 h, followed by MK-2206 for 72 h (BF65 24 h→MK-2206 72 h). As single treatment controls, cells were treated with *(R)(S)(S)*-BF65 for 24 h followed by DMSO for 72 h (BF65 24 h→DMSO 72 h) or treated with MK-2206 for 72 h (MK-2206 72 h). (C) Cells were cotreated with *(R)(S)(S)*-BF65 and MK-2206 for 96 h (BF65+MK-2206 96 h), or with either *(R)(S)(S)*-BF65 or MK-2206 alone for 96 h (BF65 96 h or MK-2206 96 h). (D) Cells were treated with MK-2206 for 24 h followed by *(R)(S)(S)*-BF65 for 72 h (MK-2206 24 h→BF65 72 h), MK-2206 for 24 h and then DMSO for 72 h (MK-2206 24 h→DMSO 72 h) or *(R)(S)(S)*-BF65 for 72 h (BF65 72 h). Cell viability was measured by the MTT assay for B-D. Data are presented as mean ± SE of three independent experiments. The differences between single treatments vs. combination treatments were assessed by 2-sided t-tests. *, $P < 0.05$; **, $P < 0.01$; ***, $P < 0.001$. (E) IC_{50} values of *(R)(S)(S)*-BF65 and MK-2206 in single or combination treatments, and CI_{50} values of the combination treatments calculated from data shown in B-D. (F) IC_{90} values of *(R)(S)(S)*-BF65 and MK-2206 in single or combination treatments and CI_{90} of the combination treatments obtained from the same experiments as described in B-D except that the SRB assay was performed to measure cell viability (data shown in Fig. 1S).

Fig. 2. *(R)(S)(S)*-BF65 and MK-2206 induce cell cycle arrest in a dose-dependent manner. (A) Cell cycle distribution at the 24 h time point. (B) The percentage of cells in G0/G1 and G2/M. SKOV3 cells were treated with various concentrations of *(R)(S)(S)*-BF65 and MK-2206 either alone or in

combination for 24 or 48 h and harvested for flow cytometric analysis. Quantitative data are presented as mean ± SE of three independent experiments.

Fig. 3. The combination of MK-2206 with *(R)(S)(S)*-BF65 results in cell cycle arrest in G0/G1 and G2/M, induction of subG1, and suppression of cells with greater than 4n DNA content induced by *(R)(S)(S)*-BF65 in SKOV3 cells. (A) Cell cycle distribution. (B) The percentage of cells in subG1. (C) The percentage of cells in G0/G1. (D) The percentage of cells in G2/M. (E) The percentage of cells with > 4n DNA content. SKOV3 cells were treated with 40 nM *(R)(S)(S)*-BF65 or 20 μM MK-2206 either alone or in combination for 6 to 96 h and harvested for flow cytometric analysis. Quantitative data are presented as mean ± SE of two or three independent experiments.

Fig. 4. Changes of protein expression patterns in SKOV3 cells induced by *(R)(S)(S)*-BF65. (A) Proteins associated with G2/M cell cycle progression. (B) Proteins associated cell death and the MAPK signaling pathway. SKOV3 cells were treated with 0, 10, 20 or 40 nM of *(R)(S)(S)*-BF65 for 24, 48, or 72 h, and harvested for Western blot analysis.

Fig. 5. Changes of protein expression patterns in SKOV3 cells induced by *(R)(S)(S)*-BF65 and MK-2206. (A) Proteins associated with G2/M cell cycle progression and the Akt signaling pathway. (B) Proteins associated cell death and the MAPK signaling pathway. SKOV3 cells were treated with 10 nM *(R)(S)(S)*-BF65 and 5 μM MK-2206 or 40 nM *(R)(S)(S)*-BF65 and 20 μM MK-2206 either alone or in combination for 24 or 48 h, and harvested for Western blot analysis.

Fig. 6. MK-2206 enhances the microtubule depolymerization effect of *(R)(S)(S)*-BF65 and vincristine. SKOV3 cells were treated with 40 nM of *(R)(S)(S)*-BF65 or vincristine, or 20 μM of MK-2206 either

alone or in combination for 24 h and then subjected to immunofluorescence staining of α-tubulin (green). The nucleus is counterstained with DAPI (blue). Cell images were captured at a magnification of 400x. Scale bar: 20 μm.

Fig. 7. The combination of MK-2206 with *(R)(S)(S)*-BF65 or vincristine significantly inhibits cell migration. (A) Wound healing cell images taken at a magnification of 100x. Scale bar = 100 μm. (B) Quantitative wound healing data obtained from at least 5 experiments. * $P < 0.05$ (combination vs. single treatments).

Figure 1

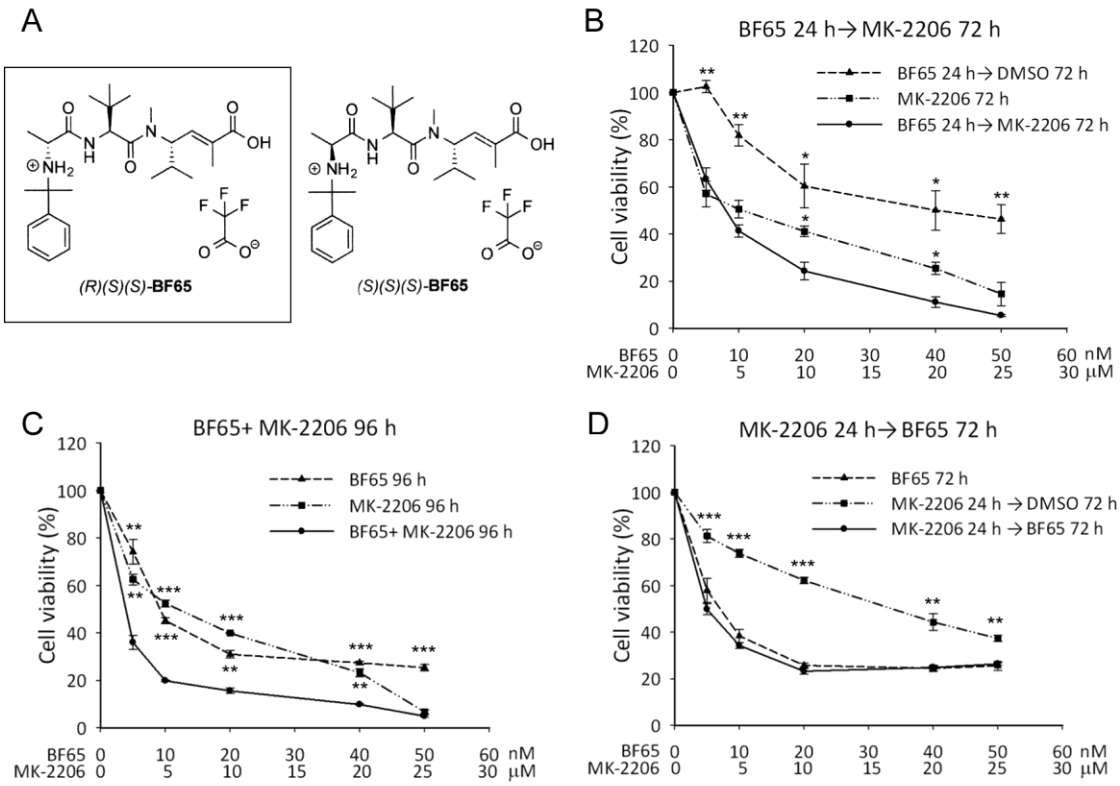

E

Treatment sequence	IC_{50} (BF65: nM, MK-2206: μM)				CI_{50}
	Single treatment		Combination treatment		
	BF65	MK-2206	BF65	MK-2206	
BF65 24 h→ MK-2206 72 h	40.1	5.18	7.6	3.8	0.92
BF65+MK-2206 96 h	8.9	5.7	3.9	1.95	0.78
MK-2206 24 h→ BF65 72 h	6.6	16.0	4.98	2.49	0.91

F

Treatment sequence	IC_{90} (BF65: nM, MK-2206: μM)				CI_{90}
	Single treatment		Combination treatment		
	BF65	MK-2206	BF65	MK-2206	
BF65 24 h→ MK-2206 72 h	55.3	14.3	7.89	3.95	0.42
BF65+ MK-2206 96 h	19.0	12.0	4.95	2.47	0.47
MK-2206 24 h→ BF65 72 h	17.0	19.9	11.2	5.60	0.94

Figure 2

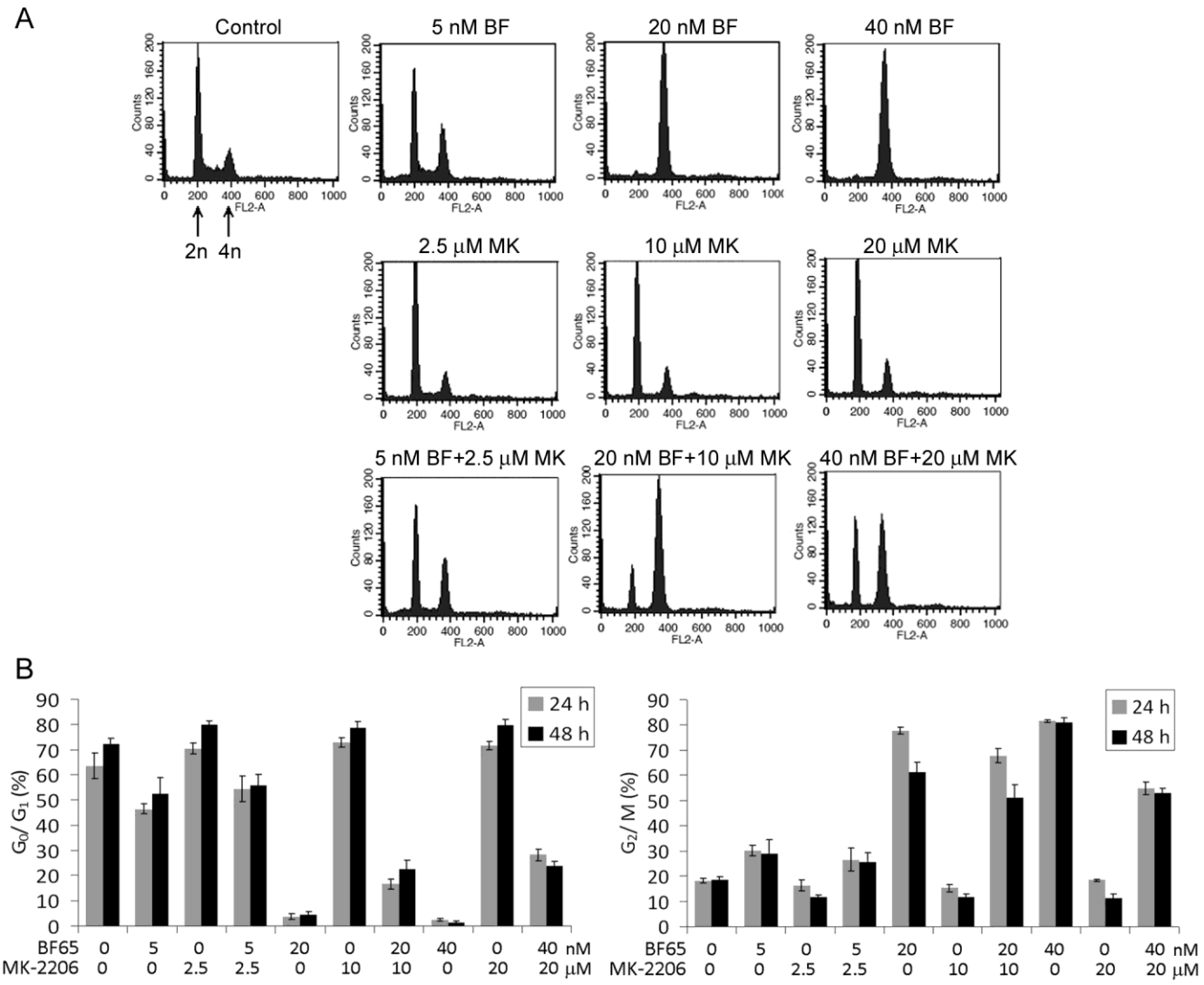
A
Control
5 nM BF
20 nM BF
40 nM BF
2.5 μM MK
10 μM MK
20 μM MK
5 nM BF+2.5 μM MK
20 nM BF+10 μM MK
40 nM BF+20 μM MK
Counts
FL2-A
2n
4n
B
24 h
48 h
G0/ G1 (%)
G2/ M (%)
BF65 0 5 0 5 20 0 20 40 0 40 nM
MK-2206 0 0 2.5 2.5 0 10 10 0 20 20 μM

Figure 3

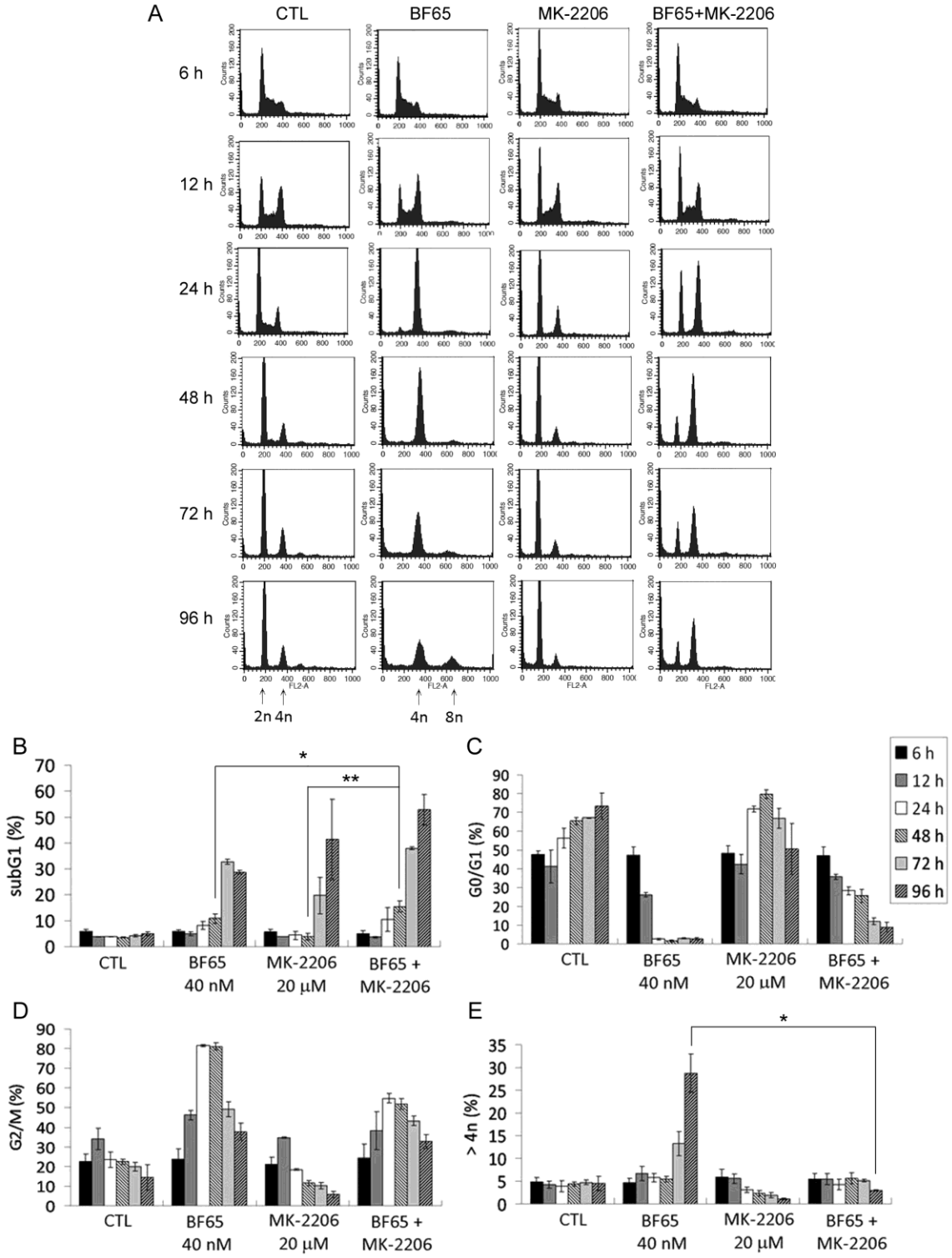
A
CTL
BF65
MK-2206
BF65+MK-2206
6 h
12 h
24 h
48 h
72 h
96 h
Counts
FL2-A
2n 4n
4n 8n
B
subG1 (%)
*
**
CTL
BF65 40 nM
MK-2206 20 µM
BF65 + MK-2206
C
G0/G1 (%)
6 h
12 h
24 h
48 h
72 h
96 h
D
G2/M (%)
E
> 4n (%)

Figure 4

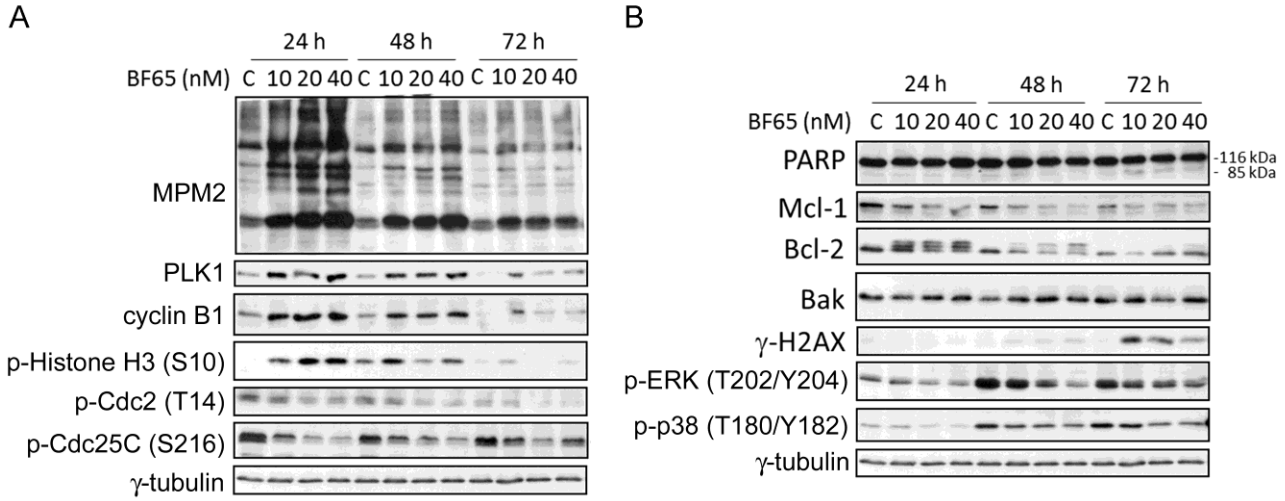

Figure 5

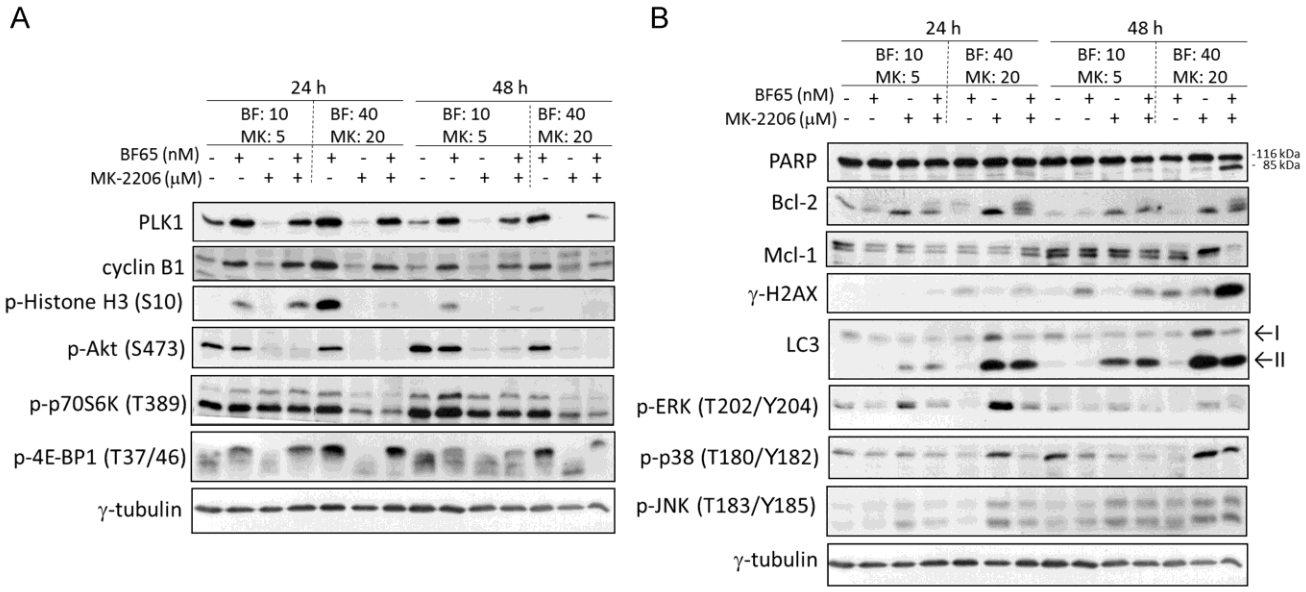

Figure 6

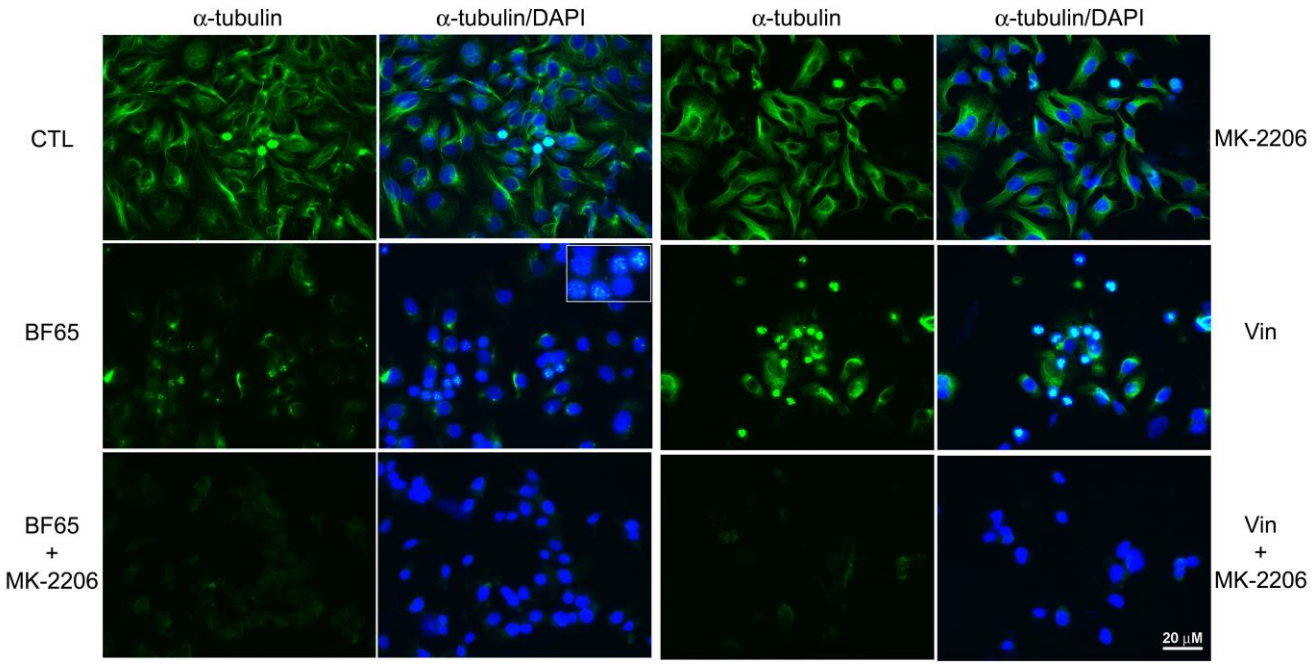
α-tubulin
α-tubulin/DAPI
α-tubulin
α-tubulin/DAPI
CTL
MK-2206
BF65
Vin
BF65
+
MK-2206
Vin
+
MK-2206
20 μM

Figure 7

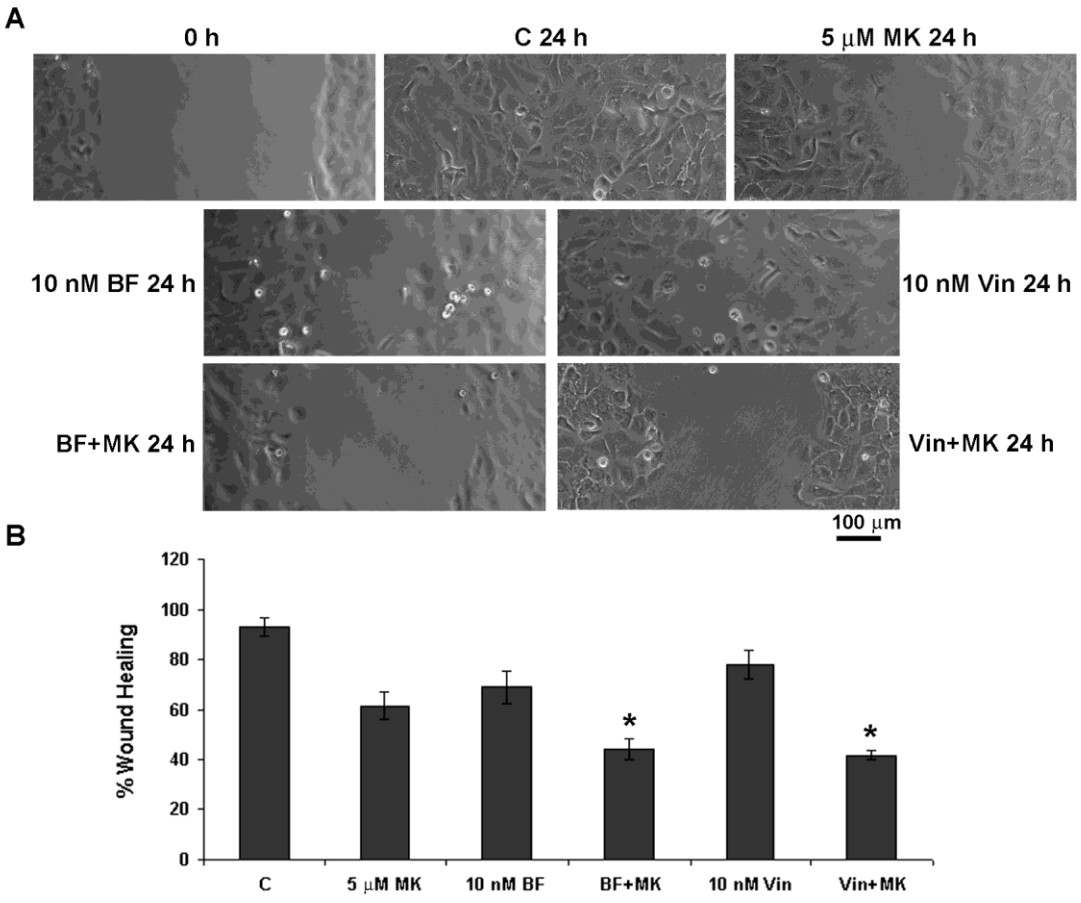
A
0 h
C 24 h
5 μM MK 24 h
10 nM BF 24 h
10 nM Vin 24 h
BF+MK 24 h
Vin+MK 24 h
100 μm
B
% Wound Healing
120
100
80
60
40
20
0
*
*
C
5 μM MK
10 nM BF
BF+MK
10 nM Vin
Vin+MK

Figure S1

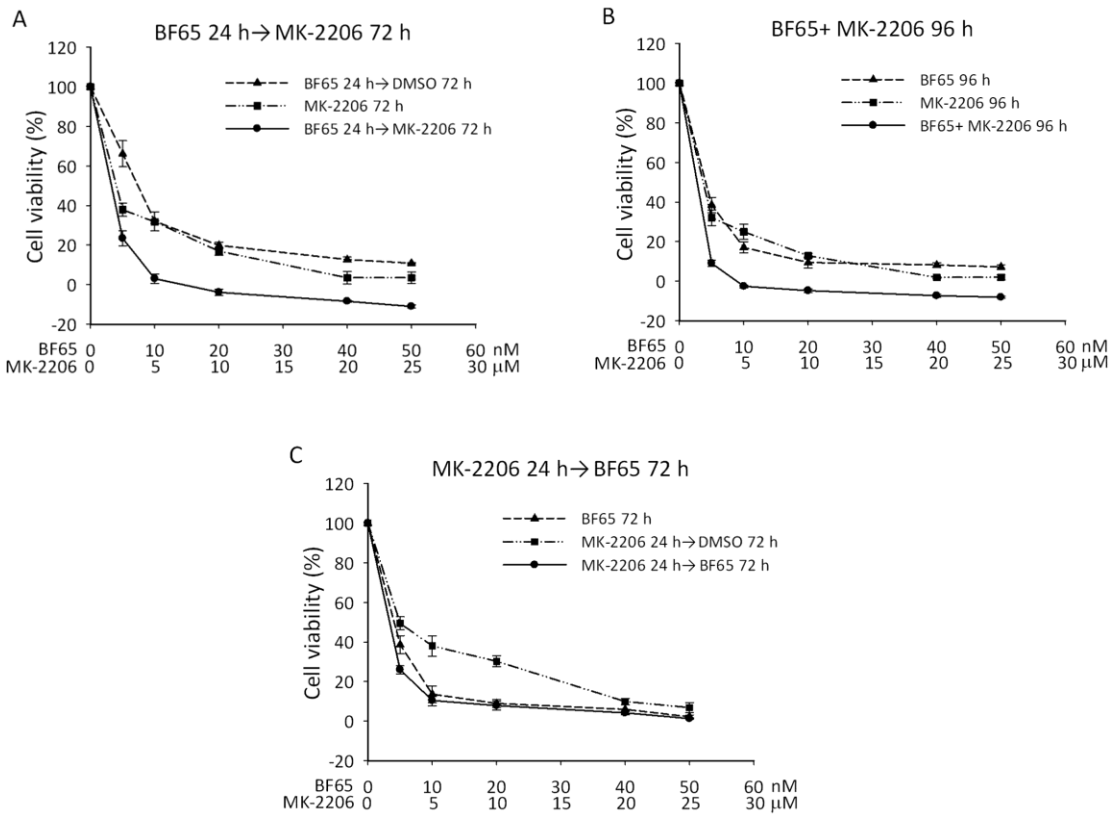

Fig. S1. The combination of *(R)(S)(S)*-BF65 and MK-2206 synergistically inhibits SKOV3 cell proliferation in three different treatment sequences. (A) Cells were treated with *(R)(S)(S)*-BF65 for 24 h, followed by MK-2206 for 72 h (BF65 24 h→MK-2206 72 h). As single treatment controls, cells were treated with *(R)(S)(S)*-BF65 for 24 h followed by DMSO for 72 h (BF65 24 h→DMSO 72 h) or treated with MK-2206 for 72 h (MK-2206 72 h). (B) Cells were cotreated with *(R)(S)(S)*-BF65 and MK-2206 for 96 h (BF65+MK-2206 96 h), or with either *(R)(S)(S)*-BF65 or MK-2206 alone for 96 h (BF65 96 h or MK-2206 96 h). (C) Cells were treated with MK-2206 for 24 h followed by *(R)(S)(S)*-BF65 for 72 h (MK-2206 24 h→BF65 72 h), MK-2206 for 24 h and then DMSO for 72 h (MK-2206 24 h→DMSO 72 h) or *(R)(S)(S)*-BF65 for 72 h (BF65 72 h). Cell viability was measured by the SRB assay. Data are presented as mean ± SE of three independent experiments. *(R)(S)(S)*-BF65 is abbreviated as BF65.

Figure S2

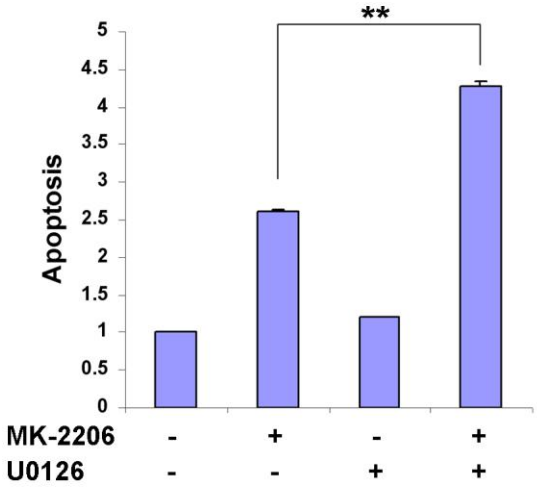

Fig. S2. MEK inhibitor U0126 enhances cell death induced by MK-2206. SKOV3 cells were pretreated with vehicle (DMSO) or 10 μM U0126, a MEK inhibitor which suppressed ERK activation, for 30 min and then treated with 20 μM MK-2206 in the presence of 10 μM U0126 for 24 h. Apoptosis was measured using the Cell Death Detection ELISA^{PLUS} kit. MK-2206-induced cell death was significantly enhanced suggesting that MK-2206-induced ERK activation is associated with cell survival.